

Sketched Equivariant Imaging Regularization and Deep Internal Learning for Inverse Problems

Guixian Xu, Jinglai Li, Junqi Tang*
School of Mathematics, University of Birmingham

J.TANG.2@BHAM.AC.UK

Abstract

Equivariant Imaging (EI) regularization has become the de-facto technique for unsupervised training of deep imaging networks, without any need of ground-truth data. Observing that the EI-based unsupervised training paradigm currently has significant computational redundancy leading to inefficiency in high-dimensional applications, we propose a sketched EI regularization which leverages the randomized sketching techniques for acceleration. We then extend our sketched EI regularization to develop an accelerated deep internal learning framework – Sketched Equivariant Deep Image Prior (Sk.EI-DIP), which can be efficiently applied for single-image and task-adapted reconstruction. Our numerical study on X-ray CT image reconstruction tasks demonstrate that our approach can achieve order-of-magnitude computational acceleration over standard EI-based counterpart in single-input setting, and network adaptation at test time.

1. Introduction

Unsupervised training has become a vital research direction for imaging inverse problems (Carioni et al., 2024; Tirer et al., 2024). For the most popular and widely applied medical imaging applications such as CT/MRI/PET, such strategies seek to train deep reconstruction network from only the noisy and incomplete measurement data:

$$y = Ax^\dagger + \varepsilon, \quad (1)$$

where we denote here $x^\dagger \in \mathbb{R}^d$ as the ground-truth image (to be estimated), $A \in \mathbb{R}^{n \times d}$ as the measurement operator, $\varepsilon \in \mathbb{R}^n$ as the measurement noise, while $y \in \mathbb{R}^n$ as the measurement data. To be more precise, such unsupervised training schemes typically seek to learn a reconstruction network (set of network parameters denoted as θ here)

$$\mathcal{F}_\theta(A^\dagger y) \rightarrow x \quad (2)$$

with only the knowledge of the measurement data y and the measurement operator A . Here we denote A^\dagger as the pseudo-inverse of A , or a stable approximation of it (such as the FBP for X-ray CT). This line of research initialized on the Deep Internal Learning schemes (see recent review paper by Tirer et al. (2024)) such as the Deep Image Prior (DIP) approach (Ulyanov et al., 2018; Tachella et al., 2021; Mataev et al., 2019; Liu et al., 2019) for learning image reconstruction from single input, and more recently the Noise2X-type approaches (Lehtinen et al., 2018; Batson and Royer, 2019), and its extension Artifact2Artifact (Liu et al., 2020). The most successful unsupervised training paradigm is currently the Equivariant Imaging (EI) regularization proposed by (Chen et al., 2021, 2022; Tachella et al., 2023), which is able to enforce the network to learn beyond the range space of the measurement operator A and fully achieve ground-truth-free training under incomplete and noisy measurements. Comparing to the standard supervised training which requires the ground-truth and measurement pairs, the unsupervised training in general, is computationally

much more costly. This is due to the fact that the forward/adjoint/pseudo-inverse operators are computed in each iteration of the training optimizer, leading to significant computational overhead. In this work, we take an initial yet crucial step for mitigating the computational limitation of unsupervised training schemes for deep imaging networks, by accelerating EI regularization via dimensionality reduction (sketching) techniques rooted in stochastic optimization. We apply the sketched EI regularizer first in the internal learning setting, which can be view as an EI-regularized DIP. Our numerical study in X-ray CT image reconstruction demonstrates that our proposed Sketched EI-DIP can achieve order-of-magnitude acceleration over standard EI-regularized DIP under this single-input internal learning setting, as well as the network-adaptation task in test time.

1.1 Background

Deep Internal Learning. The most typical and fundamental deep internal learning scheme is the deep imaging prior (DIP) approach proposed by (Ulyanov et al., 2018). The DIP can be described as approximately minimizing the following loss by first-order optimizers such as SGD or Adam:

$$\begin{aligned}\theta^* &\approx \arg \min_{\theta} \|y - A\mathcal{F}_{\theta}(z)\|_2^2, \\ x^* &= \mathcal{F}_{\theta^*}(z),\end{aligned}\tag{3}$$

where the input z can be chosen as random vector or $z = A^\dagger y$ for warm-starting (Tachella et al., 2021). In its vanilla form, it takes an randomly initialized deep convolutional network and train it directly on the given single measurement data. Perhaps surprisingly, the vanilla version of DIP can already provide excellent reconstruction performance on many inverse problems such as image denoising/superresolution/deblurring and tomographic image reconstruction tasks such as CT/MRI/PET (Singh et al., 2023; Mayo et al., 2024).

Apart from learning reconstruction from a single input, DIP can also be effectively applied for network adaptation at test time against distribution shifts (Barbano et al., 2022). Suppose given a pretrained reconstruction network on a certain set of measurements y and operator A , if we apply directly the network to a different inverse problem with a new A' which have fewer measurements and noisier y' , the pretrained network can perform badly. However, one can mitigate this distribution shift by adapting the network via the DIP framework above or regularized versions of DIP such as the DIP-GSURE approach by Abu-Hussein et al. (2022).

Equivariant Imaging Regularization. Among all the unsupervised approaches for training deep imaging networks, EI framework proposed by Chen et al. (2021, 2022) was the first to address explicitly the issue of learning beyond the range space of the forward operator A utilizing the inherent symmetric structures of the imaging systems. Given a collection of measurements Y , and group transformation T_g tailored for the imaging systems (for example, rotation for CT), the vanilla EI framework can be written as:

$$\theta^* \approx \arg \min_{\theta} f_{\text{EI}}(\theta) := \underbrace{\mathbb{E}_{g \sim G, y \sim Y} \{\|y - A(\mathcal{F}_{\theta}(A^\dagger y))\|_2^2\}}_{\text{MC loss}} + \lambda \underbrace{\|T_g \mathcal{F}_{\theta}(A^\dagger y) - \mathcal{F}_{\theta}(A^\dagger A T_g \mathcal{F}_{\theta}(A^\dagger y))\|_2^2}_{\text{EI regularization}},\tag{4}$$

where the first term is the measurement-consistency loss, while the second term is the EI regularizer which enable the training program to learn in the null-space of A . After this first pivoting work, variants of EI has been developed for enhancing robustness to measurement noise, using additional G-SURE (Chen et al., 2022) or UNSURE (Tachella et al., 2024) regularizer alongside with EI. Meanwhile, extensions of EI on new group actions tailored for different inverse problems have been proposed (Wang and Davies, 2024b,a; Scanvic et al., 2023). In our work we focus on sketching the vanilla form of EI regularizer but the same principle can be easily extended for all these enhanced versions of EI.

Randomized Sketching and Stochastic Optimization. Operator sketching and stochastic gradient-based optimization techniques has been widely applied for machine learning (Kingma and Ba, 2015; Johnson and Zhang, 2013; Pilanci and Wainwright, 2015, 2017; Tang et al., 2017) and more recently in imaging inverse problems (Sun et al., 2019; Ehrhardt et al., 2024). In the context of imaging inverse problems, given a measurement consistency loss $\arg \min_x \|Ax - y\|_2^2$, one can split the objective function into N partition of minibatches: $\|Ax - y\|_2^2 = \sum_{i=1}^N \|M_i Ax - M_i y\|_2^2$, where M_i are the set of sketching operators (typically sub-sampling for imaging applications). After splitting the objective function into minibatches, one can use stochastic gradient methods as the optimizer for efficiency. In a pioneering work of Tang et al. (2020), they demonstrate that the success of stochastic optimization and operator sketching techniques depends on the spectral structure of the forward operator A . If A has a fast decay on the singular-value spectrum, then we can expect order-of-magnitude acceleration in terms of computational complexity over deterministic methods such as proximal gradient descent or FISTA (Beck and Teboulle, 2009). Most of the computationally intensive imaging inverse problems fall into this category, for example, X-ray CT, multi-coil MRI and Positron Emission Tomography all admit efficient applications of operator sketching and stochastic optimization. In our work here, we leverage operator sketching for the acceleration of EI-regularization and jointly with the DIP measurement consistency.

1.2 Contributions

The contribution of our work is three-fold:

- **Sketched EI regularization** – We propose an efficient variant of the EI regularizer, mitigating the computational inefficiency of the original approach by (Chen et al., 2021).
- **Theoretical analysis of sketched EI** – We provide a motivational theoretical analysis on the approximation bound of our sketched EI regularizer, demonstrating that our approach admits a nice mathematical interpretation.
- **Sketched EI-DIP and application in X-ray CT** – Based on our Sketched EI regularizer, jointly with sketching on measurement consistency term, we propose an efficient deep internal learning framework, namely the Sk.EI-DIP, for single-input and task-adapted image reconstruction. We apply our Sk.EI-DIP approach in sparse-view X-ray CT imaging tasks and demonstrate significant computational acceleration over standard DIP and EI-regularized DIP.

2. Sketched Equivariant Imaging Regularization and Deep Internal Learning

In this section, we present our sketching scheme for the EI regularizer, and the resulting Sketched EI-DIP approach for single-input deep internal learning. Meanwhile, we provide a theoretical analysis revealing the motivation of this scheme for additional insights.

2.1 Algorithmic Framework

The EI-regularized unsupervised learning is much more computationally inefficient comparing to supervised training, due to the need of computing the measurement operator multiple times in every training iterations. Observing that there is significant computational redundancy in the EI-regularizer, we propose a sketched EI regularizer, which replace A and A^\dagger with sketched minibatches $A_M := MA$ and $A_M^\dagger := (MA)^\dagger$, where

$M \in \mathbb{R}^{m \times d}$ is a random sketching operator satisfying $\mathbb{E}(M^T M) = I$. In imaging inverse problems, we can simply choose M to be a sub-sampling operator:

$$\|T_g \mathcal{F}_\theta(A^\dagger y) - \mathcal{F}_\theta(A_M^\dagger A_M T_g \mathcal{F}_\theta(A^\dagger y))\|_2^2 \approx \|T_g \mathcal{F}_\theta(A^\dagger y) - \mathcal{F}_\theta(A^\dagger A T_g \mathcal{F}_\theta(A^\dagger y))\|_2^2. \quad (5)$$

Jointly performing the sketch in the DIP measurement consistency term with $y_M := My$, we can derive our Sketched EI-DIP as follows:

$$\theta^* \approx \arg \min_{\theta} f_{\text{Sk.EI-DIP}}(\theta) := \mathbb{E}_{g \sim G, M} \left\{ \underbrace{\|y_M - A_M(\mathcal{F}_\theta(A^\dagger y))\|_2^2}_{\text{Sketched MC loss}} + \lambda \underbrace{\|T_g \mathcal{F}_\theta(A^\dagger y) - \mathcal{F}_\theta(A_M^\dagger A_M T_g \mathcal{F}_\theta(A^\dagger y))\|_2^2}_{\text{Sketched EI regularization}} \right\}, \quad (6)$$

Then taking $x^* = \mathcal{F}_{\theta^*}(A^\dagger y)$ we obtain the desired output. Here A^\dagger and A_M^\dagger are stable approximations of pseudo-inverses, for example, the filtered-backprojection (FBP) for X-ray CT imaging. In practice, we can always precompute $A^\dagger y$, and also predefine a set of N sketching operators M_1, M_2, \dots, M_N . In each of training iteration of SGD or Adam, we randomly sample a M_i where $i \in [1, N]$ and compute an efficient approximate gradient. For structured inverse problems such as X-ray CT, we can observe significant computational acceleration via this form of sketching.

2.2 Theoretical Analysis

For a proof-of-concept, we provide following bound for the proposed sketching scheme, demonstrating that our sketched EI regularizer is an effective approximation of the original EI.

Theorem 1 (Approximation bound for Sketched EI regularization) *Suppose the network \mathcal{F}_θ is L -Lipschitz, while $\|v\|_2 \leq r$, we have:*

$$\|v - \mathcal{F}_\theta(A^\dagger A v)\|_2 - Lr\delta \leq \|v - \mathcal{F}_\theta(A_M^\dagger A_M v)\|_2 \leq \|v - \mathcal{F}_\theta(A^\dagger A v)\|_2 + Lr\delta \quad (7)$$

almost surely, where δ is a constant only depending on the sketch size m and the choice of sketching operator, and we denote here $v := T_g \mathcal{F}_\theta(A^\dagger y)$.

We provide the proof of this theorem in the appendix. The L -Lipschitz continuity assumption of the form:

$$\|\mathcal{F}_\theta(p) - \mathcal{F}_\theta(q)\|_2 \leq L\|p - q\|_2, \quad \forall p, q \in \mathcal{X} \quad (8)$$

on the reconstruction network \mathcal{F}_θ is standard for the theoretical analysis of deep networks in imaging inverse problems. For example, in the convergence analysis of plug-and-play algorithms (Ryu et al., 2019; Tan et al., 2024) and diffusion-based MCMC (Cai et al., 2024), such type of assumptions have been used on the pretrained denoisers or generative image priors based on deep networks for the convergence proofs. The theorem above provides a upper bound and lower bound sandwiching the sketched EI regularization with original EI regularization, with a deviation δ which scales approximately as $O(1/\sqrt{m})$.

This theoretical result, although preliminary and motivational, justifies that the proposed sketching scheme provides a good approximation for original EI regularizer statistically, and admits a nice mathematical interpretation.

3. Numerical Experiments

In this section, we show numerically the performance of the proposed method for the sparse-view CT image reconstruction problem.

3.1 Setup and Implementation

We evaluate the proposed approach on *sparse-view CT image reconstruction* problem, where the forward operator A is underdetermined with a nontrivial null-space ($m < n$). Specifically, the imaging physics model of X-ray computed tomography (CT) is the discrete radon transform, and the physics model A is the radon transformation where 50 views (angles) are uniformly subsampled to generate the sparse-view sinograms (observations) y . The Filtered back projection (FBP) function, *i.e.* `iradon`, is used to perform a stable approximation of A^\dagger .

The aim of this task is to recover a ground truth image x^* from a single observation y . We incorporate the invariance of the CT images to rotations into the deep image prior scheme, and \mathcal{G} is the group of rotations from 1 to 360 degrees ($|\mathcal{G}| = 360$). We use a single data sampled from the CT100 dataset (Clark et al., 2013), and resize it to 256×256 pixels, then we apply the `radon` function on it to generate the 50-views sinogram.

Throughout the experiments, we use a U-Net (Ronneberger et al., 2015) to build \mathcal{F}_θ as suggested in Chen et al. (2021). We compare our method (Sketched EI-DIP) with two different learning strategies: unsupervised deep image prior approach with the loss function (3); unsupervised deep image prior term with the equivariance regularized term (EI-DIP) as showed in (4). For a fair comparison with sketched EI-DIP, we use the residual U-Net architecture for all the counterpart learning methods to ensure all methods have the same inductive bias from the neural network architecture.

We demonstrate that the sketched operation is straightforward and can be easily extended to existing deep models without modifying the architectures. All our experiments were performed using a NVIDIA RTX 3050ti GPU, alongside with `DeepInv` toolbox¹. All the compared methods are implemented in PyTorch and optimized by Adam (Kingma and Ba, 2015), for which we set the learning rate to 5×10^{-4} . We train all of the comparing methods over 5,000 iterations.

3.2 Numerical Results

We conduct a comparative numerical study of our proposed Sketched EI-DIP method against traditional method such as the DIP, as well as the deep image prior with state-of-the-art equivariant regularizer (Chen et al., 2021), EI-DIP. To ensure a fair comparison, all parameters involved in the deep image prior and EI method are either manually tuned to optimality or automatically selected as described in the referenced papers. For our Sketched EI-DIP, we choose subsampling sketch as our M , which split the measurement operator into N minibatches, $A_{M_1}, A_{M_2} \dots A_{M_N}$ from interleaved angles. We test on the choices $N = 2, 3, 4, 5$ respectively here. We present our results with detailed descriptions in the following figures which demonstrate the effectiveness of our sketched EI scheme.

1. <https://deepinv.github.io/deepinv/>

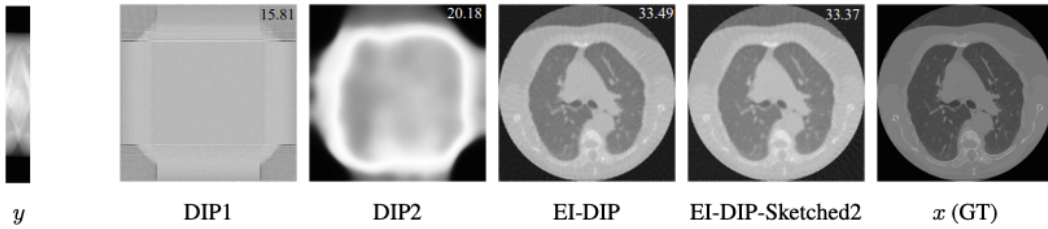


Figure 1: Images reconstructed by DIP, EI-DIP and our Sketched EI-DIP. We can observe that the DIP approach performs badly in our experiments (DIP-1 uses UNet while DIP-2 employs an Auto-Encoder network achitecture). With the help of EI-regularizer, the EI-DIP approach can provide much more improved reconstruction. Our Sketched EI-DIP performs as good as EI-DIP.

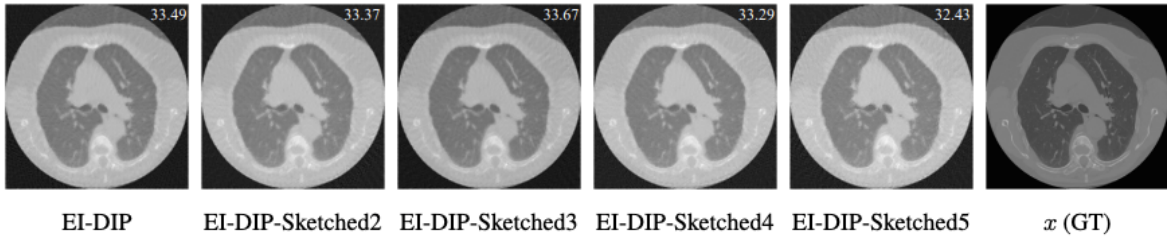


Figure 2: Images reconstructed by Sketched EI-DIP, with different sketch sizes. The sketching is performed increasingly more aggressive from left to right, and we can observe that the results for Sketched EI-DIP is nearly the same (sometimes even better) than full EI-DIP, for the number of minibatch split chosen to be either $N = 2, 3$ or 4 . The result would deteriorate if we choose to sketch over aggressively, say $N = 5$, indicating a phase-transition.

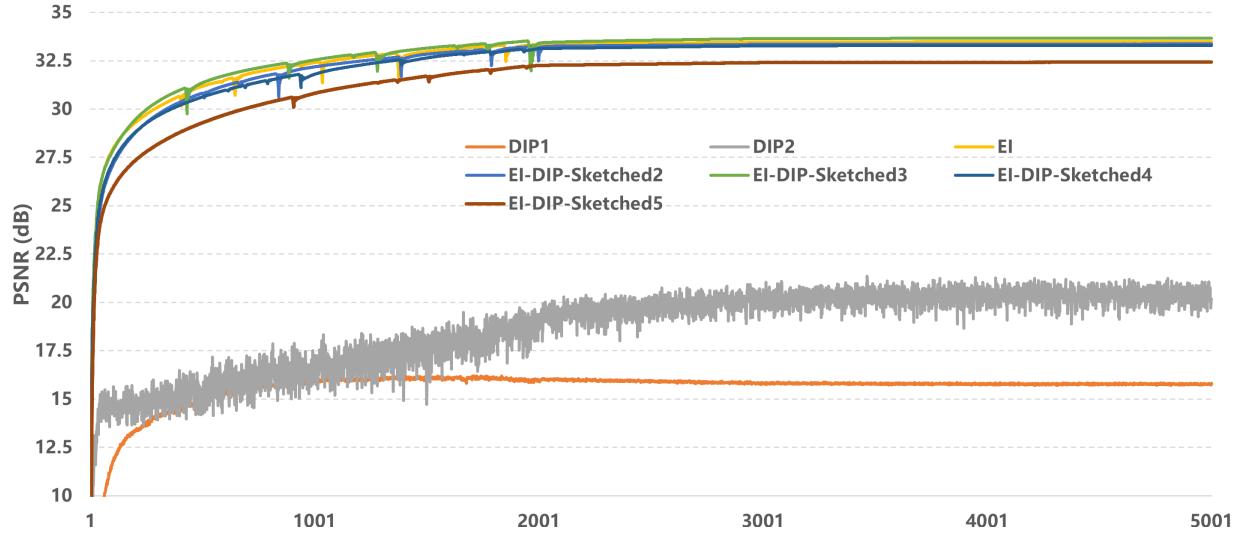


Figure 3: Reconstruction accuracy curves for all the compared schemes. We can observe that, for the case where the minibatch split number to be 2, 3 or 4, the Sketched EI-DIP converges to the same accuracy comparing to full EI-DIP, with the same convergence speed (yet the computational time is massively reduced).

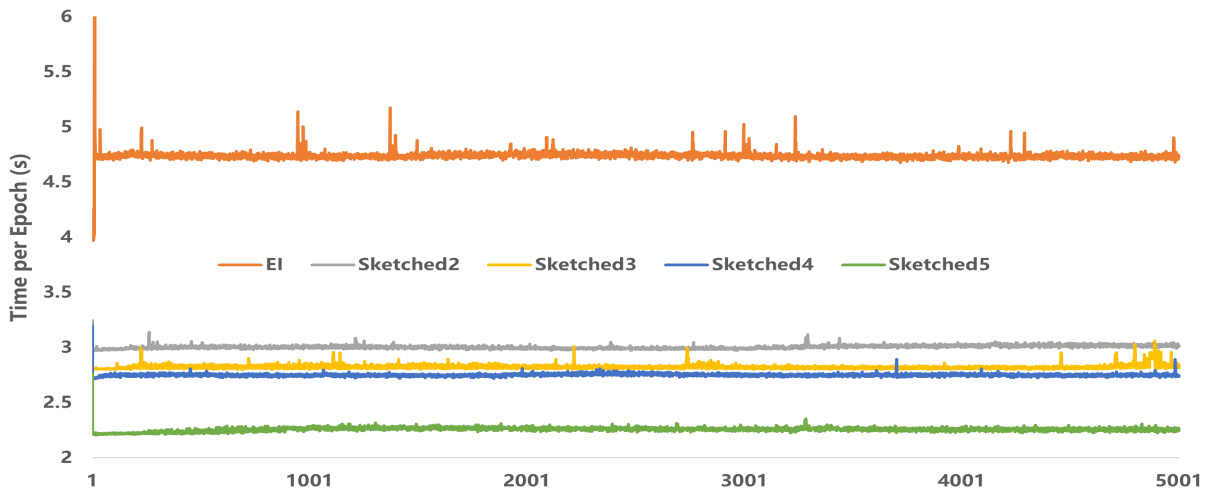


Figure 4: Execution time comparison between EI-DIP and Sketched EI-DIP at each iteration. We can observe that our scheme can achieve significant computational acceleration over full EI-DIP.

4. Conclusion

In this work we propose a sketched EI regularizer which can be efficiently applied for unsupervised training of deep imaging networks, especially in the deep internal learning setting with single input. We provide a motivational theoretical analysis of the proposed sketching scheme demonstrating that it is an effective approximation of the original EI regularization proposed by [Chen et al. \(2021\)](#). In single-input setting, we

compare our Sketched EI-DIP approach with standard DIP and EI-DIP for sparse-view X-ray CT imaging tasks, and observe a substantial acceleration. Our work has focused on sketching the vanilla form of EI, nevertheless, it is obvious that this scheme can be trivially applied to its enhanced versions such as REI (Chen et al., 2022; Tachella et al., 2024).

5. Appendix

In this appendix we provide the proof for the motivational bound presented in Theorem 1 for the approximation of EI regularizer. We start by proving the upper bound:

$$\begin{aligned} \|v - \mathcal{F}_\theta(A_M^\dagger A_M v)\|_2 &= \|v - \mathcal{F}_\theta(A_M^\dagger A_M v) + \mathcal{F}_\theta(A^\dagger A v) - \mathcal{F}_\theta(A^\dagger A v)\|_2 \\ &\leq \|v - \mathcal{F}_\theta(A^\dagger A v)\|_2 + \|\mathcal{F}_\theta(A_M^\dagger A_M v) - \mathcal{F}_\theta(A^\dagger A v)\|_2. \end{aligned} \quad (9)$$

Due to the assumption on the L -Lipschitz continuity of the network, we have

$$\begin{aligned} &\|\mathcal{F}_\theta(A_M^\dagger A_M v) - \mathcal{F}_\theta(A^\dagger A v)\|_2 \\ &\leq L \|A_M^\dagger A_M v - A^\dagger A v\|_2 \\ &\leq L \|A^\dagger M^\dagger M A - A^\dagger A\|_2 \|v\|_2 \\ &\leq L \|A^\dagger (M^T M - I) A\|_2 \|v\|_2 \\ &\leq L r \|A^T (M^T M - I) A\|_2 \end{aligned} \quad (10)$$

The remaining challenge is to bound the term $\|A^T (M^T M - I) A\|_2 \leq \delta$ almost surely, which actual value is dependent on the choice of sketching operator M . Here we illustrate with the choice of sub-Gaussian sketches, while subsampling and randomized orthogonal sketches also satisfy the bound with different value of δ and probability. According to (Pilanci and Wainwright, 2015, Proposition 1), if M is a σ -sub-Gaussian sketch with sketch size m , we have:

$$L r \|A^T (M^T M - I) A\|_2 \leq L r \delta, \quad (11)$$

with:

$$\delta = c_0 \sqrt{\frac{d}{m}} + \delta_0 \quad (12)$$

with probability at least $1 - \exp(-c_1 \frac{m \delta_0^2}{\sigma^4})$ where c_0, c_1 are universal constants. We hence finish the proof of the upper bound. For the lower bound, we use the same reasoning:

$$\begin{aligned} \|v - \mathcal{F}_\theta(A^\dagger A v)\|_2 &= \|v - \mathcal{F}_\theta(A_M^\dagger A_M v) + \mathcal{F}_\theta(A_M^\dagger A_M v) - \mathcal{F}_\theta(A^\dagger A v)\|_2 \\ &\leq \|v - \mathcal{F}_\theta(A_M^\dagger A_M v)\|_2 + \|\mathcal{F}_\theta(A_M^\dagger A_M v) - \mathcal{F}_\theta(A^\dagger A v)\|_2 \\ &\leq \|v - \mathcal{F}_\theta(A_M^\dagger A_M v)\|_2 + L r \delta \end{aligned} \quad (13)$$

Then immediately we have $\|v - \mathcal{F}_\theta(A_M^\dagger A_M v)\|_2 \geq \|v - \mathcal{F}_\theta(A^\dagger A v)\|_2 - L r \delta$. Thus finishes the proof.

References

- Shady Abu-Hussein, Tom Tirer, Se Young Chun, Yonina C Eldar, and Raja Giryes. Image restoration by deep projected gsure. In *Proceedings of the IEEE/CVF Winter Conference on Applications of Computer Vision*, pages 3602–3611, 2022.
- Riccardo Barbano, Johannes Leuschner, Maximilian Schmidt, Alexander Denker, Andreas Hauptmann, Peter Maass, and Bangti Jin. An educated warm start for deep image prior-based micro ct reconstruction. *IEEE Transactions on Computational Imaging*, 8:1210–1222, 2022.
- Joshua Batson and Loic Royer. Noise2self: Blind denoising by self-supervision. In *International Conference on Machine Learning*, pages 524–533, 2019.
- A. Beck and M. Teboulle. Fast gradient-based algorithms for constrained total variation image denoising and deblurring problems. *IEEE Transactions on Image Processing*, 18(11):2419–2434, 2009.
- Ziruo Cai, Junqi Tang, Subhadip Mukherjee, Jinglai Li, Carola-Bibiane Schönlieb, and Xiaoqun Zhang. Nf-ula: Normalizing flow-based unadjusted langevin algorithm for imaging inverse problems. *SIAM Journal on Imaging Sciences*, 17(2):820–860, 2024.
- Marcello Carioni, Subhadip Mukherjee, Hong Ye Tan, and Junqi Tang. Unsupervised approaches based on optimal transport and convex analysis for inverse problems in imaging. *Radon Series on Computational and Applied Mathematics*, 2024.
- Dongdong Chen, Julián Tachella, and Mike E Davies. Equivariant imaging: Learning beyond the range space. In *Proceedings of the IEEE/CVF International Conference on Computer Vision*, pages 4379–4388, 2021.
- Dongdong Chen, Julián Tachella, and Mike E Davies. Robust equivariant imaging: a fully unsupervised framework for learning to image from noisy and partial measurements. In *Proceedings of the IEEE/CVF Conference on Computer Vision and Pattern Recognition*, pages 5647–5656, 2022.
- Kenneth Clark, Bruce Vendt, Kirk Smith, John Freymann, Justin Kirby, Paul Koppel, Stephen Moore, Stanley Phillips, David Maffitt, Michael Pringle, et al. The cancer imaging archive (tcia): maintaining and operating a public information repository. *Journal of digital imaging*, 26:1045–1057, 2013.
- Matthias J Ehrhardt, Zeljko Kereta, Jingwei Liang, and Junqi Tang. A guide to stochastic optimisation for large-scale inverse problems. *arXiv preprint arXiv:2406.06342*, 2024.
- Rie Johnson and Tong Zhang. Accelerating stochastic gradient descent using predictive variance reduction. In *Advances in neural information processing systems*, pages 315–323, 2013.
- Diederik P Kingma and Jimmy Ba. Adam: A method for stochastic optimization. *Proceedings of 3rd International Conference on Learning Representations*, 2015.
- Jaakko Lehtinen, Jacob Munkberg, Jon Hasselgren, Samuli Laine, Tero Karras, Miika Aittala, and Timo Aila. Noise2noise: Learning image restoration without clean data. *arXiv preprint arXiv:1803.04189*, 2018.

- Jiaming Liu, Yu Sun, Xiaojian Xu, and Ulugbek S Kamilov. Image restoration using total variation regularized deep image prior. In *ICASSP 2019-2019 IEEE International Conference on Acoustics, Speech and Signal Processing (ICASSP)*, pages 7715–7719. Ieee, 2019.
- Jiaming Liu, Yu Sun, Cihat Eldeniz, Weijie Gan, Hongyu An, and Ulugbek S Kamilov. Rare: Image reconstruction using deep priors learned without groundtruth. *IEEE Journal of Selected Topics in Signal Processing*, 14(6):1088–1099, 2020.
- Gary Mataev, Peyman Milanfar, and Michael Elad. Deepred: Deep image prior powered by red. In *Proceedings of the IEEE/CVF International Conference on Computer Vision Workshops*, pages 0–0, 2019.
- Perla Mayo, Matteo Cencini, Carolin M Pirkl, Marion I Menzel, Michela Tosetti, Bjoern H Menze, and Mohammad Golbabaee. Stodip: Efficient 3d mrf image reconstruction with deep image priors and stochastic iterations. In *International Workshop on Machine Learning in Medical Imaging*, pages 128–137. Springer, 2024.
- M. Pilanci and M. J. Wainwright. Randomized sketches of convex programs with sharp guarantees. *Information Theory, IEEE Transactions on*, 61(9):5096–5115, 2015.
- Mert Pilanci and Martin J Wainwright. Newton sketch: A near linear-time optimization algorithm with linear-quadratic convergence. *SIAM Journal on Optimization*, 27(1):205–245, 2017.
- Olaf Ronneberger, Philipp Fischer, and Thomas Brox. U-net: Convolutional networks for biomedical image segmentation. In Nassir Navab, Joachim Hornegger, William M. Wells, and Alejandro F. Frangi, editors, *Medical Image Computing and Computer-Assisted Intervention – MICCAI 2015*, pages 234–241, Cham, 2015. Springer International Publishing. ISBN 978-3-319-24574-4.
- Ernest Ryu, Jialin Liu, Sicheng Wang, Xiaohan Chen, Zhangyang Wang, and Wotao Yin. Plug-and-play methods provably converge with properly trained denoisers. In *International Conference on Machine Learning*, pages 5546–5557, 2019.
- Jérémy Scanvic, Mike Davies, Patrice Abry, and Julián Tachella. Self-supervised learning for image super-resolution and deblurring. *arXiv preprint arXiv:2312.11232*, 2023.
- Imraj Singh, Riccardo Barbano, Zeljko Kereta, Bangti Jin, Kris Thielemans, and Simon Arridge. 3d pet-dip reconstruction with relative difference prior using a sirf-based objective. Fully3D, 2023.
- Yu Sun, Brendt Wohlberg, and Ulugbek S Kamilov. An online plug-and-play algorithm for regularized image reconstruction. *IEEE Transactions on Computational Imaging*, 2019.
- Julián Tachella, Junqi Tang, and Mike Davies. The neural tangent link between cnn denoisers and non-local filters. *IEEE/CVF Conference on Computer Vision and Pattern Recognition*, 2021.
- Julián Tachella, Dongdong Chen, and Mike Davies. Sensing theorems for unsupervised learning in linear inverse problems. *Journal of Machine Learning Research*, 24(39):1–45, 2023.
- Julián Tachella, Mike Davies, and Laurent Jacques. Unsure: Unknown noise level stein’s unbiased risk estimator. *arXiv preprint arXiv:2409.01985*, 2024.
- Hong Ye Tan, Subhadip Mukherjee, Junqi Tang, and Carola-Bibiane Schönlieb. Provably convergent plug-and-play quasi-newton methods. *SIAM Journal on Imaging Sciences*, 17(2):785–819, 2024.

- Junqi Tang, Mohammad Golbabaee, and Mike E Davies. Gradient projection iterative sketch for large-scale constrained least-squares. In *International Conference on Machine Learning*, pages 3377–3386. PMLR, 2017.
- Junqi Tang, Karen Egiazarian, Mohammad Golbabaee, and Mike Davies. The practicality of stochastic optimization in imaging inverse problems. *IEEE Transactions on Computational Imaging*, 6:1471–1485, 2020.
- Tom Tirer, Raja Giryes, Se Young Chun, and Yonina C Eldar. Deep internal learning: Deep learning from a single input. *IEEE Signal Processing Magazine*, 41(4):40–57, 2024.
- Dmitry Ulyanov, Andrea Vedaldi, and Victor Lempitsky. Deep image prior. In *Proceedings of the IEEE Conference on Computer Vision and Pattern Recognition*, pages 9446–9454, 2018.
- Andrew Wang and Mike Davies. Fully unsupervised dynamic mri reconstruction via diffeo-temporal equivariance. *arXiv preprint arXiv:2410.08646*, 2024a.
- Andrew Wang and Mike Davies. Perspective-equivariant imaging: an unsupervised framework for multi-spectral pansharpening. *arXiv preprint arXiv:2403.09327*, 2024b.